Arq Neuropsiquiatr 2008;66(1):64-68

DIFFUSION-WEIGHTED MR IMAGES AND PINEOBLASTOMA

Diagnosis and follow-up

Emerson L. Gasparetto[1], L. Celso Hygino da Cruz Jr[2], Thomas M. Doring[3], Bertha Araújo[4], Mário Alberto Dantas[5], Leila Chimelli[6], Romeu C. Domingues[7]

Abstract – Pineoblastomas are uncommon pineal tumors, which demonstrate rapid growing and poor prognosis. We report the case of a 43-year-old man with an enhancing pineal region mass, which showed restriction of the diffusion on diffusion-weighted (DW) MR images. The surgical biopsy defined the diagnosis of pineoblastoma and the therapy was initiated with radiation and chemotherapy. Three months later, the follow-up MR imaging showed areas suggestive of necrosis and the DW images demonstrate no significant areas of restricted diffusion. The differential diagnosis of pineal region masses that could show restriction of diffusion is discussed.

KEY WORDS: pineoblastoma, magnetic resonance imaging, diffusion-weighted imaging.

Imagens pesadas em difusão e pineoblastoma: diagnóstico e acompanhamento

Resumo – Pineoblastomas são tumores incomuns da glândula pineal, os quais têm crescimento rápido e prognóstico reservado. Os autores objetivam relatar o caso de um homem de 43 anos de idade com uma massa na região pineal com realce pelo contraste, a qual demonstrou restrição da difusão nas imagens de ressonância magnética (RM) pesadas em difusão. A biópsia cirúrgica definiu o diagnóstico de pineoblastoma e o tratamento foi iniciado com radio e quimioterapia. Três meses mais tarde, a RM de controle demonstrou áreas sugestivas de necrose e não mais eram observadas áreas de restrição da difusão da água. O diagnóstico diferencial das massas na região pineal que podem apresentar restrição da difusão é discutido.

PALAVRAS-CHAVE: pineoblastoma, ressonância magnética, imagens pesadas em difusão.

Pineal parenchymal neoplasms account for less than 15% of all pineal region masses. The pineoblastoma is the malignant variant, composed of undifferentiated or immature cells. This lesion is unencapsulated and often invades directly into the adjacent brain or may spread through the CSF[1,2]. Regarding the imaging findings, CT scans may show a pineal mass with calcification and contrast enhancement. The MR images demonstrate a lesion hypo- or iso-intense on T1- and hyperintense on T2-weighted images, with heterogeneous enhancement after gadolinium administration. However, there is a considerable overlap of the imaging findings of pineoblastomas and pineocytomas[1-3]. The diffusion-weighted (DW) MR imaging provides information about the movement of the water molecules along random pathways. Many factors may cause restriction of water diffusion in living tissues, such as cellular compartmentalization, cell type and number, cell membrane density, and macromolecule size and type[4]. Several authors have studied the application of DW images in brain neoplasms, trying to discriminate tumour tissue from oedema, cyst or necrosis, and even trying to access tumour cellularity and grading[5,6]. However, to our knowledge, the DW imaging findings of pineoblastomas were not previously assessed.

We present the DW imaging findings of a patient with pineoblastoma, with emphasis to the differential diagnosis and follow-up features.

METHOD

A 43-year-old man presented with severe headaches. The neurological and laboratorial investigations were unremarkable.

[1,2,3,7]Clinics Multi-Imagem and CDPI - Clínica de Diagnóstico por Imagem; [6]Diagnose - Laboratory of Pathology; [4,5]Oncoclínica and Departments of [1]Radiology and [6]Pathology, University of Rio de Janeiro, Rio de Janeiro RJ, Brazil.

Received 27 July 2007, received in final form 9 October 2007. Accepted 8 November 2007.

Dr. Emerson L. Gasparetto – Rua Lopes Trovão 88 / 1702B - 24220-071 Niterói RJ - Brasil. E-mail: egasparetto@gmail.com

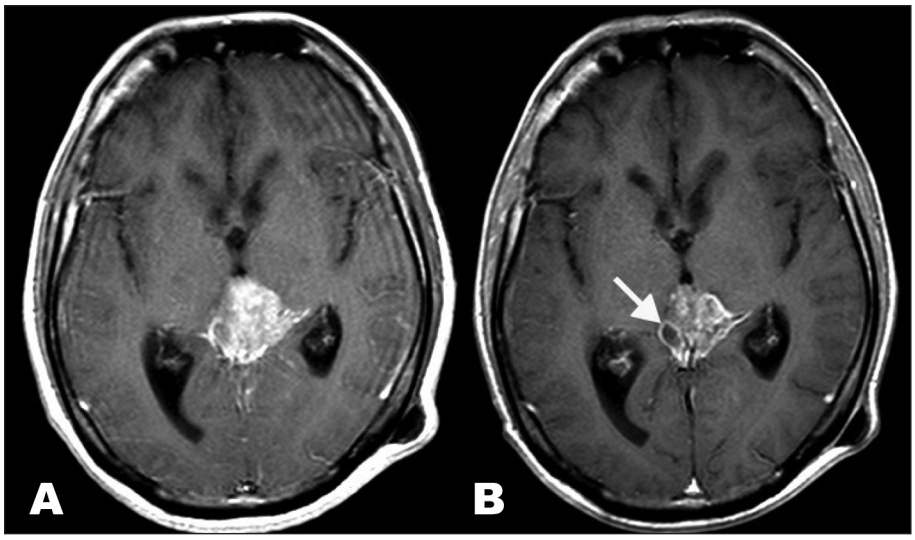

Fig 1. T1-weighted MR image pre-treatment (A) shows an enhancing pineal mass. The post-treatment T1-weighted MR image (B) demonstrates the pineal region mass with heterogeneous enhancement, presenting areas suggestive of necrosis (arrow).

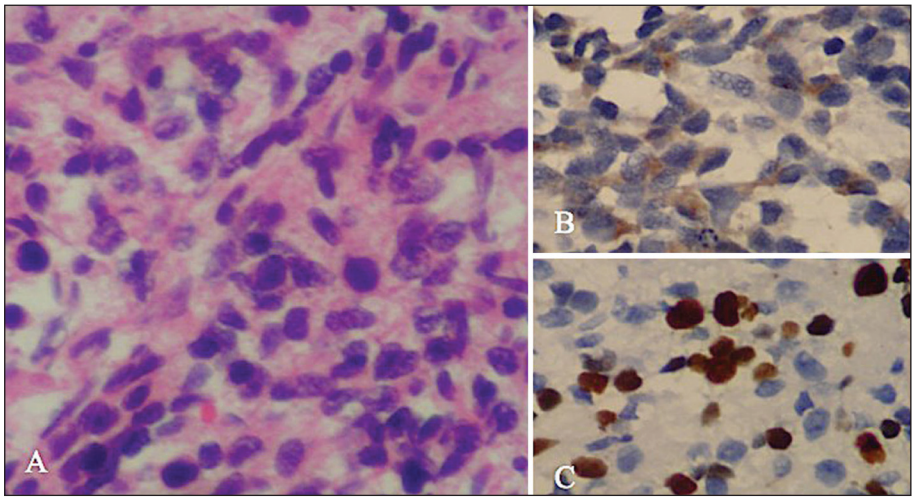

Fig 2. Hematoxylin and eosin staining of the tumor specimen demonstrates undifferentiated neoplastic cells with nuclear atypias (A). The neoplastic cells were immunoreactive to synaptophysin (B) and demonstrated high proliferative level on KI-67 (C; 400x).

MR imaging protocol

Brain MR imaging was performed in a 1.5T scanner (Avanto; Siemens, Erlangen, Germany) with standard technique (T1-weighted images before and after intravenous contrast administration [repetition time (TR)=350 ms, echo time (TE)=7.8 ms, matrix= 256x256 and section thickness=5 mm), T2-weighed images (TR=3540 ms, TE=106 ms, matrix=320x320 and section thickness=3 mm) and fluid-attenuation inversion-recovery (FLAIR) sequence (TR=9650 ms, TE=87 ms, inversion time=2500 ms, matrix= 256x256 and section thickness=5 mm)]. In addition, a diffusion-weighted sequence was also obtained (TR=2900 ms, TE=84 ms, matrix=128x128, section thickness=6 mm). The diffusion gradients were applied along the x, y, and z axes and the DW imaging sequence was acquired with 3 different b values (b=0, b=500 and 1000 s/mm^2).

MR imaging findings before treatment

On the pineal region, there was a 3.0x3.0x2.5 cm^3 mass with heterogeneous signal, predominantly low on T1- and high on T2-weighted images. After intravenous gadolinium administration, intense heterogeneous enhancement was seen (Fig 1A). In addition, there was enhancement on the tentorium and cerebellar sulci. Also, the lesion was compressing the cerebral aqueduct, resulting in moderated hydrocephalus, which was shunted. The DW images demonstrated high signal in most of the lesion, with low signal on the ADC maps.

Diagnosis and treatment

The patient underwent surgical biopsy and the histological sections showed a tumour with very high cellularity, com-

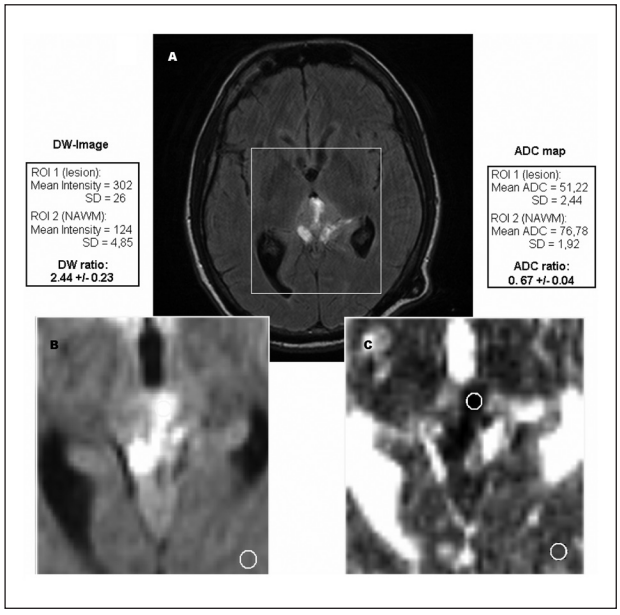

Fig 3. MR Imaging before treatment: (A) FLAIR demonstrates the hyperintense pineal mass. (B) DW image shows high signal in the lesion and a DW ratio of 2.43. (C) ADC map confirms the area of restricted diffusion and a mean ADC ratio of 0.67.

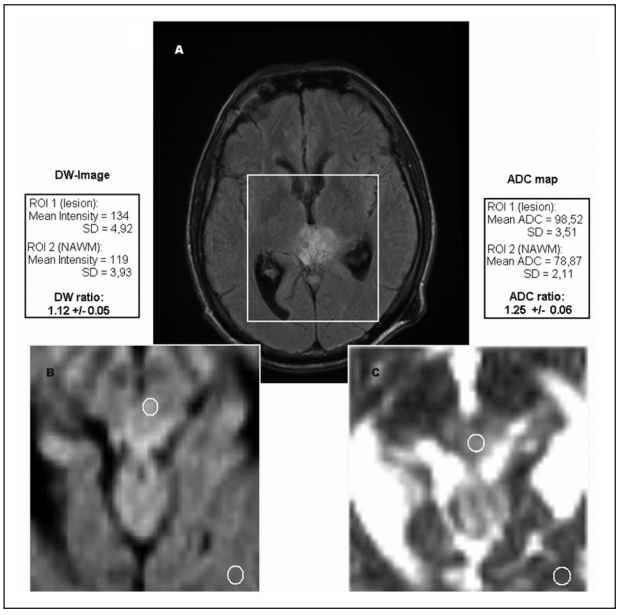

Fig 4. MR imaging after treatment: (A) FLAIR image demonstrates the hyperintense pineal mass. (B) DW image shows discrete high signal and a DW ratio of 1.12. (C) ADC map demonstrates increased mean ADC ratio (1.25).

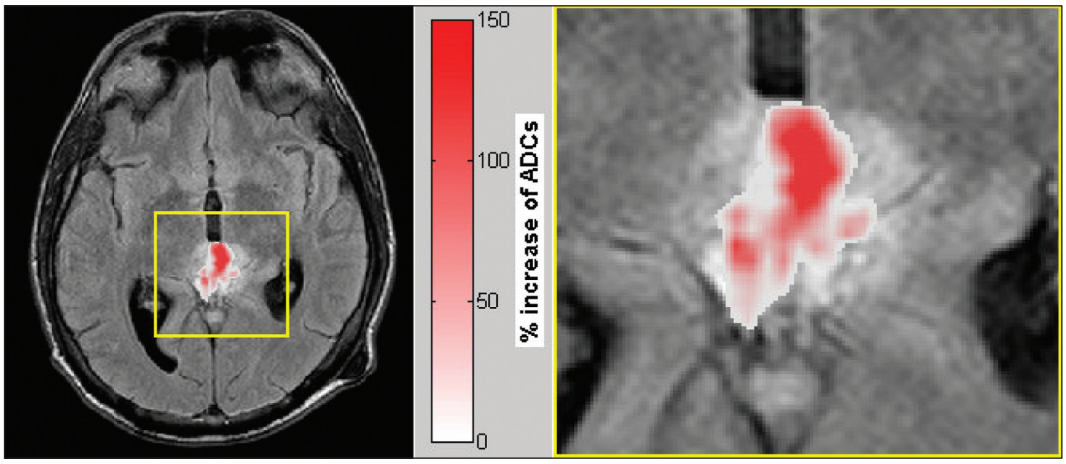

Fig 5. Percentual change of ADCs in necrotic area of lesion pre- and post-treatment with underlay of the corresponding FLAIR image: histogram analysis of this area yields a mean percentual increase of 67% and a maximum increase of 142% in the ADC values.

posed of undifferentiated neoplastic cells with nuclear atypias. The neoplastic cells were immunoreactive to synaptophysin and demonstrated high proliferative index on KI-67 (Fig 2). The diagnosis of pineoblastoma was then confirmed and the treatment was started with radiation and chemotherapy (vincristine).

MR imaging findings after treatment

Three months after the beginning of the treatment, a follow-up MR imaging study was performed with the same previous protocol. At that time, written informed consent for the publication of the case was obtained. For post-processing reasons, to reduce effects of misregistration coming from different positioning before and after treatment, the same technician carefully positioned the slices when adjusting the scan protocol. The follow-up MR imaging showed a lesion with similar dimensions, but with large areas of very low signal on T1-, high signal on T2-weighted images and peripheral enhancement, suggesting necrosis (Fig 1B). These areas demonstrated slight high signal on DW images and ADC maps, corroborating the hypothesis of necrosis.

Imaging post-processing and analysis

Post-processing and analysis of the images were performed with standard software (Syngo VB11, Siemens, Erlangen, Germany). Apparent diffusion coefficient (ADC) maps were calculated

using the diffusion-weighted datasets with the three different b-values applying linear regression methods according to the following matrix equation: {ln[I(b)]=ln [I(b_0)]–ADCxb}]. Considering the images at the same slice position, ln means the natural logarithm, I(b) the corresponding image of a b-value, I(b_0) the image without diffusion-weighting (b=0). The angular coefficient of the resulting curve was considered to be the ADC.

Both, the qualitative DW images (b=1000 s/mm²), where an intensity value is assigned to each pixel, and the quantitative ADC maps, where the local ADC represents each pixel value, were used for a statistical region-of-interest based analysis.

In the DW images as well as in the ADC maps, one region of interest (ROI1) was positioned in the lesion and a second one (ROI2) was placed in the normal-appearing white matter (NAWM). Mean DW values, mean ADCs and their standard deviation (SD) and ratios ([DW ratio=DW_{lesion} intensity/DW_{NAWM} intensity] and [ADC ratio=ADC_{lesion}/ADC_{NAWM}]) were calculated before and after treatment. Furthermore, the statistical significance for the difference of ADCs of the measurements before and after treatment was assessed.

In the pre-treatment MR images, using the mean intensity values and mean ADCs for ROI1 and ROI2 on DW images and ADC maps, it was found a DW ratio of 2.43 and an ADC ratio 0.67, respectively (Fig 3). In the post-treatment MR images, the same measurements yielded a DW ratio of 1.12 and a ADC ratio of 1.25 (Fig 4). Comparing the ADC ratios before and after treatment, there was a significant difference ($p<0.001$).

In addition, to visualize the alteration of the ADC values after treatment, it was calculated a map of percentual-change on a voxel-based approach. In the first step the dataset of ADC maps before and after treatment were co-registered to each other using the software Statistical Parametric Mapping (SPM5) (Welcome Department of Imaging Neuroscience, London, UK)[7,8]. Then, for every pixel the percentual increase of ADC was estimated using the equation [(ADC_{post}–ADC_{pre})/ADC_{pre}x100%], where ADC_{pre} describes the ADC before treatment and ADC_{post} after treatment.

The percentual-change-map (Fig 5) shows clearly that there is an increase of ADCs up to ~140 % after treatment.

DISCUSSION

The pineal parenchymal tumours are the most common neoplasms in the pineal gland, except for the germ cell tumour. The World Health Organization classification subcategorizes the pineal parenchymal tumour into three classes: pineocytoma, pineoblastoma, and pineal parenchymal tumour of intermediate differentiation[2,8]. Compared to pineocytoma, pineoblastoma is characterized by early onset (first two decades vs third or fourth decades), infiltration into surrounding structures, primitive neuroectodermal cell composition, presence of Homer-Wright or Flexner-Wintersteiner rosettes, frequent brain metastasis or spinal seeding and worse prognosis (five-year survival rate: 58% vs 86%)[1-3,9]. Our patient had 43 years at the time of the diagnosis, but demonstrated subarachnoid spread and histological findings confirming the diagnosis of pineoblastoma.

Several authors have studied the diffusion-weighted MR imaging in patients with intracranial tumours[6,10-13]. Stadnik et al.[10] studied the DW images of 20 patients with intracranial tumors. The gliomas, meningiomas and metastases showed no restriction of water movement, but this feature was seen in two cases of lymphoma. Krabbe et al.[6] also investigated the DW images aspects in patients with the same types of tumour. They showed that the ADC of cerebral metastases was higher than of high grade gliomas. Yamasaki et al.[11] studied different types of brain tumours, emphasizing the diffusion-weighted MR imaging findings. They suggested that ADC is useful for differentiation of some brain tumours. In the present case, the pineoblastoma showed restriction of water diffusion at the time of the diagnosis, demonstrating high signal on DW images and low signal on ADC maps.

The potential applications of DW MR imaging in measurement of the response of solid tumours to therapy have been assessed. The results of studies of animal models have suggested that significant changes in water diffusion evolving in the first few weeks after initiation of treatment may be helpful in predicting response to therapy[6]. The same has been seen in patients with brain tumours. In a study of patients with glioma treated with radiation and chemotherapy, cases with stable disease showed higher ADC in tumour at one month after radiation therapy than did those in whom tumour recurred[13]. One study of six patients with brain tumours, mostly metastases, showed that ADC values in the tumours measured approximately one week after therapy increased significantly in responders, compared with ADC values in nonresponders[13]. In the present case, the ratio between the ADC values in the tumour and normal appearing white matter was 0.67 at the time of the diagnosis and 1.25 three months later, after the treatment.

In conclusion, pineoblastoma may show restriction of water diffusion, which might be related to its high cellularity. In addition, this case illustrates very well the treatment response of the lesion based on the DW images. Future studies investigating the DW images features of the remaining lesions that occur in the pineal region can define the rule on this image sequence in the differential diagnosis of pineal regions masses.

REFERENCES

1. Reis F, Faria AV, Zanardi VA, Menezes JR, Cendes F, Queiroz LS. Neuroimaging in pineal tumors. J Neuroimaging 2006;16:52-58.
2. Smirniotopoulos JG, Rushing EJ, Mena H. Pineal region masses: differential diagnosis. Radiographics 1992;12:577-596.

3. Nakamura M, Saeki N, Iwadate Y, Sunami K, Osato K, Yamaura A. Neuroradiological characteristics of pineocytoma and pineoblastoma. Neuroradiology 2000;42:509-514.
4. Hagmann P, Jonasson L, Maeder P, Thiran JP, Wedeen VJ, Meuli R. Understanding diffusion mr imaging techniques: from scalar diffusion-weighted imaging to diffusion tensor imaging and beyond. Radiographics 2006;26(Suppl):S205-S223.
5. Krabbe K, Gideon P, Wagn P, Hansen U, Thomsen C, Madsen F. MR diffusion imaging of human intracranial tumours. Neuroradiology 1997;39:483-489.
6. Provenzale JM, Mukundan S, Barboriak DP. Diffusion-weighted and perfusion MR imaging for brain tumor characterization and assessment of treatment response. Radiology 2006;239:632-649.
7. Ashburner J, Friston K. Multimodal image coregistration and partitioning a unified framework. NeuroImage 1997;6:209-217.
8. Mardor Y, Pfeffer R, Spiegelmann R, et al. Early detection of response to radiation therapy in patients with brain malignancies using conventional and high b-value diffusion-weighted magnetic resonance imaging. J Clin Oncol 2003;21:1094-1100.
9. Song K, Nasim M, Agarwal R, Benardete E. Pathologic quiz case: a 15-year-old girl with an intracranial midline mass. Pineoblastoma, World Health Organization Grade IV. Arch Pathol Lab Med 2004;128:707-708.
10. Stadnik TW, Chaskis C, Michotte A, et al. Diffusion-weighted MR imaging of intracerebral masses: comparison with conventional MR imaging and histologic findings. Am J Neuroradiol 2001;22:969-976.
11. Yamasaki F, Kurisu K, Satoh K, et al. Apparent diffusion coefficient of human brain tumors at MR imaging. Radiology 2005;235:985-991.
12. Kono K, Inoue Y, Nakayama K, et al. The role of diffusion-weighted imaging in patients with brain tumors. AJNR Am J Neuroradiol 2001; 22: 1081-1088.
13. Hein PA, Eskey CJ, Dunn JF, Hug EB. Diffusion-weighted imaging in the follow-up of treated high-grade gliomas: tumor recurrence versus radiation injury. Am J Neuroradiol 2004;25:201-209.